Biochemical and Biophysical Research Communications 425 (2012) 806–811

Contents lists available at SciVerse ScienceDirect

Biochemical and Biophysical Research Communications

journal homepage: www.elsevier.com/locate/ybbrc

Crystal structure of *Plasmodium falciparum* thioredoxin reductase, a validated drug target

Giovanna Boumis [a], Giorgio Giardina [a], Francesco Angelucci [c], Andrea Bellelli [a,b], Maurizio Brunori [a,b], Daniela Dimastrogiovanni [a,1], Fulvio Saccoccia [a], Adriana E. Miele [a,*]

[a] Department of Biochemical Sciences and Istituto Pasteur – Fondazione Cenci Bolognetti, "Sapienza" University of Rome, 00185 Rome, Italy
[b] CNR Institute of Molecular Pathology and Biology, "Sapienza" University of Rome, 00185 Rome, Italy
[c] Department of Life, Health and Environmental Sciences, University of L'Aquila, 67010 L'Aquila, Italy

ARTICLE INFO

Article history:
Received 27 July 2012
Available online 6 August 2012

Keywords:
Malaria
Thiol-mediated redox metabolism
Thioredoxin reductase
Protein crystallography
Rational drug design

ABSTRACT

Plasmodium falciparum is the vector of the most prevalent and deadly form of malaria, and, among the *Plasmodium* species, it is the one with the highest rate of drug resistance. At the basis of a rational drug design project there is the selection and characterization of suitable target(s). Thioredoxin reductase, the first protection against reactive oxygen species in the erythrocytic phase of the parasite, is essential for its survival. Hence it represents a good target for the design of new anti-malarial active compounds. In this paper we present the first crystal structure of recombinant *P. falciparum* thioredoxin reductase (PfTrxR) at 2.9 Å and discuss its differences with respect to the human orthologue. The most important one resides in the dimer interface, which offers a good binding site for selective non competitive inhibitors. The striking conservation of this feature among the *Plasmodium* parasites, but not among other Apicomplexa parasites neither in mammals, boosts its exploitability.

1. Introduction

Malaria, one of the major threats for human health worldwide, is endemic in more than 100 countries, mainly in tropical and subtropical areas, and causes about 1 million human deaths per year. It represents a huge socioeconomic burden in developing countries, where limited access to therapy has also the drawback of increasing the reservoir of infectivity [1].

Malaria is a vector borne disease caused by the unicellular Apicomplexan parasite belonging to the genus *Plasmodium*. There are four main species infecting humans, and among them *Plasmodium falciparum* is the most deadly and also the one with the highest rate of drug resistance [1].

Plasmodium has a complex developmental cycle, which includes a continuous expansion inside host erythrocytes. Therefore it is exposed to high fluxes of reactive oxygen species (ROS), while maintaining a reduced intracellular environment. As a defense mechanism, the parasite evolved a complex network of NADPH-dependent redox enzymes: a complete glutathione (GSH) system and a specialized thioredoxin (Trx) system. The first one comprises GSH, GSH reductase, glutaredoxin (Grx) and Grx-like proteins, GSH-S-transferase (GST), gamma-glutamylcysteine synthetase (gamma-GCS), and a GSH-dependent glyoxalase system. The second system includes Trx reductase (TrxR), several Trxs and Trx-like proteins, and Trx-dependent peroxidases [2–4]. In addition *Plasmodium* can hijack redox proteins from the host. Overall, this proved a winning strategy for survival, despite the lack of catalase and glutathione peroxidase [5].

Using genetic and chemical tools, it was demonstrated that TrxR, the first step of the thioredoxin redox cycle, and gamma-GCS, the rate-limiting step of glutathione synthesis, are essential for parasite survival [3,6]. Therefore some of the enzymes involved in this antioxidant defense pattern represent good targets for the design of new anti-malarial active compounds [7,8]. Indeed PfTrxR is a particularly attractive candidate because of its structural and functional peculiarities: namely, the presence of an extension at the N-terminus and the lack of a selenocysteine in the redox centre at the C-terminus. This last feature is common to all the Apicomplexan TrxRs, where a CGGGKCG stretch replace the GCUC stretch of mammalian TrxRs [9].

Basic to a rational drug design research project there is a thorough functional and structural characterization of a selected target that should display unique features for specificity. In this paper we

Abbreviations: PfTrxR, *Plasmodium falciparum* thioredoxin reductase; HsTrxR, homo sapiens thioredoxin reductase; Trx, thioredoxin; GSH, reduced glutathione; NADPH, nicotinamide adenine dinucleotide phosphate; FAD, flavin adenine dinucleotide; DTNB, 5,5′-dithio-bis (2-nitrobenzoic acid); Tris/HCl, Tris(hydroxymethyl)aminomethane hydrochloride.

* Corresponding author. Address: Department of Biochemical Sciences, "Sapienza" University of Rome, P.le Aldo Moro 5, 00185 Rome, Italy. Fax: +39 064440062.
E-mail address: adriana.miele@uniroma1.it (A.E. Miele).
[1] Present address: Department of Biochemistry, University of Cambridge, Cambridge CB2 1GA, UK.

0006-291X/$ - see front matter © 2012 Elsevier Inc. All rights reserved.
http://dx.doi.org/10.1016/j.bbrc.2012.07.156

present the first crystal structure of *P. falciparum* thioredoxin reductase (PfTrxR) at 2.9 Å, and discuss its properties in light of the similarities/differences with respect to human TrxR (HsTrxR, PDB ID: 2ZZC [10]), and to computer models of PfTrxR [11,12]. The crystallographic structure unveiled some significant peculiarities of the *Plasmodium* enzyme, which are discussed in terms of their exploitability for drug design.

2. Materials and methods

2.1. Expression and purification

The gene corresponding to PfTrxR (Primary accession number Q25861) was synthesized and optimized for expression in *Escherichia. coli* cells by GeneArt (Life Technologies), and was cloned into pGEX-4T-1 (GE Healthcare) expression vector, *via* BamHI and XhoI restriction sites.

The protein fused to GST-tag was expressed in BL21(DE3) bacterial cells upon induction with 0.5 mM IPTG, 20 μM FAD, incubating overnight at 16 °C. Cells were lysed by sonication in lysis buffer [0.1 M Tris/HCl, 0.4 M NaCl, pH 7.4, 5 mM β-mercaptoethanol, 5% glycerol, 10 μg/ml DNase, a cocktail of protease inhibitors (COMPLETE, Roche) and 2 mM EDTA]. The protein was purified from the soluble fraction by affinity chromatography on Glutathione Sepharose (QIAGEN). Successful expression of PfTrxR was confirmed by SDS–PAGE, highlighting a band at approximately 86 kDa (Figure not shown). The GST-tag was cleaved by thrombin (Sigma–Aldrich) that was finally removed passing the fractions on a 1 ml benzamidine FF (HS) column (GE Healthcare). The expression gave a yield of 7 mg/L culture, with a good FAD incorporation, according to the Abs_{280}/Abs_{340} ratio (data not shown).

Purified PfTrxR was exchanged into crystallization buffer (25 mM Tris/HCl, 0.2 M NaCl, pH 7.4, 5 mM β-mercaptoethanol), and concentrated to 3.5 mg/mL by ultrafiltration (Millipore), aliquoted, and stored at −20 °C.

2.2. Crystallization

Crystallization conditions were initially screened by robot (Phoenix, ArtRobbins) and then optimized by standard hanging drop methods. Crystals of PfTrxR grew over 1 month in a drop composed by 1 μl protein (3.5 mg/mL) and 1 μl well solution (16% (w/v) PEG 4000, 0.1 M Tris/HCl, pH 8.5, 0.2 M sodium acetate).

2.3. Data collection, processing, and refinement

Diffraction data have been collected on BL14.1 (HZB BESSY II electron storage ring of Berlin-Adlershof, Germany [13]) from a crystal diffracting up to 2.9 Å. Data were indexed and processed with XDS [14]. Phases were determined by molecular replacement using Phaser [15] within the CCP4 Suite [16,17], taking mitochondrial mouse TrxR as a model (PDB entry: 1ZKQ, 46% identity [18]).

The structure was refined using REFMAC5 [19] and fitted to generated electron density maps by Coot [20]. MolProbity [21] and ProCheck [22] were used to assess the quality of the final model. Data collection and refinement statistics are summarized in Table 1.

Figures were prepared with CCP4MG [23]. All the sequence alignments were made with ClustalW2 [24] available on the EBI website (http://www.ebi.ac.uk/Tools/msa/clustalw2/).

2.4. Functional assays

2.4.1. DTNB reduction assay

5,5′-dithio-bis (2-nitrobenzoic acid) (DTNB) reduction assay was performed by adding PfTrxR (5–500 nM) to a mixture of 100 mM potassium phosphate pH 7.0, 2 mM EDTA, 0.2–5.0 mM DTNB, and 300 μM NADPH at 20 °C. The increase in absorbance at 412 nm was monitored (ε_{412} = 13.6 mM^{-1} cm^{-1}) [25].

Table 1
Summary of data collection and refinement statistics for 4B1B.

Data collection	
Space group	$P2_12_12_1$
Cell dimensions: *a*, *b*, *c* (Å)	63.12, 109.18, 182.39
Resolution range (Å) (last shell)	15.7–2.9 (3.07–2.90)
R_{merge} (last shell)	0.19 (0.76)
$I/\sigma I$ (last shell)	9.23 (2.02)
Completeness (%)	96.7 (92.7)
Multiplicity	5.1 (4.4)
No. total reflections	137765
No. unique reflections	27908
Refinement	
Resolution (Å)	15.7–2.9
No. reflections used	26474
R factor	0.26
R_{free}	0.29
No. atoms	6848
Protein	6739
Ligand	109
B-Wilson ($Å^2$)	52.2
B-factor ($Å^2$)	34.25
Model quality	
R.m.s deviations	
Bond lengths (Å)	0.002
Bond angles (°)	0.39
Chiral volume ($Å^2$)	0.028
Ramachandran plot (%)	
Favored	99.7
Generously allowed	0.3
Disallowed	0

2.4.2. Insulin reduction assay

The classical turbidimetric assay [26] was performed by following the precipitation of insulin at 650 nm after addition of 300 nM PfTrxR to a reaction mixture composed of 100 mM potassium phosphate pH 7.0, 2 mM EDTA, 300 μM NADPH, 200 μM insulin, and 10 μM thioredoxin from *Schistosoma mansoni*. Stock solutions of insulin were prepared according to [26]. The parameters used to express the enzymatic activity were the starting time of precipitation and the precipitation rate (ΔAbs_{650} min^{-1}).

3. Results

3.1. The crystal structure

PfTrxR crystals belong to space group $P2_12_12_1$, with two monomers per asymmetric unit, in agreement with the dimeric active form of the enzyme [5]. Crystal diffraction at 2.9 Å allowed the resolution of the overall fold, which is superimposable to that of other members of the class-I pyridine nucleotide-disulfide oxidoreductase family. PfTrxR is a homodimeric enzyme, whose monomer has three domains: a NADPH binding domain, a FAD binding domain, and a monomer–monomer interface. It possesses three redox centers: (i) the non covalently bound FAD, which takes up electron from NADPH; (ii) the first di-thiol couple Cys88–Cys93, which takes up electrons from the isoalloxazine ring of FAD; (iii) the second di-thiol couple Cys535–Cys540 at the end of the C-terminal arm. The enzyme is an obligate dimer since the C-term Cys couple of one monomer is in close contact with the FAD Cys couple of the adjacent one, from which it takes up electrons to subsequently reduce the macromolecular substrate Trx.

All the secondary structure elements, the active site in the proximity of FAD (Supplementary material Fig. 1), the NADPH binding

pocket and the interface domain are clearly visible in the electron density map (Fig. 1).

The FAD active site is conserved, its binding mode being essentially identical to that of the mammalian enzymes. The only notable peculiarity is around the adenosine ring next to the surface, where Lys74, Leu160 and Asp319 in PfTrxR correspond, respectively, to Thr45, Tyr131 and Cys296 in HsTrxR.

Although PfTrxR was crystallized without NADPH, its binding pocket, formed by segments Gly229–Val233, Arg253–Phe260 and Ile314–Arg316, is well structured, being a canonical Rossman's fold; thus a molecule of NADPH, docked for a better localization of this domain in Fig. 1C, fits very well.

The delay in obtaining an experimental structure of such a key enzyme points to the difficulty in growing well diffracting crystals. In fact the prediction server XtalPred [27] highlighted an intrinsic low propensity to crystallize. We can now infer that this is due to the presence of three natively unstructured regions, which are not visible in the electron density map, namely (i) the N-terminal arm residues 1–37, (ii) the loop 428–456, and (iii) the C-terminal residues 506–541. The N-terminal arm, which was predicted to be unstructured by Psipred server [28] (Supplementary material Fig. 2) is characteristic of TrxR from other *Plasmodium* and Apicomplexa species (though not conserved) but is absent in mammalian TrxR (Supplementary material Fig. 3). At the C-terminus, the electron density map is well defined only up to Cys505, after which the polypeptide chain is disordered and thus non visible. This is not entirely unexpected, since the role of this C-terminal loop is to shuttle electrons from Cys88–Cys93 facing FAD to the macromolecular acceptor Trx *via* the active couple Cys535–Cys540. The topologically corresponding region, visible in the human enzyme, is shown for comparison in Fig. 2.

The long insertion loop 428–456, preceded and followed by β-strands and predicted to contain two short helices and coiled segments (Supplementary material Fig. 2), is 14 residues longer than the corresponding one in the mammalian enzymes (Supplementary material Fig. 3). Unlike the N- and C-termini, whose electron density is completely missing, in this region small volumes of electron density are present, although it is not possible to unequivocally assign them either to the backbone or to side chains. Hence this highly flexible loop can assume an ensemble of different conformations, possibly originating the spots of electron density. Therefore residues 428–456 were not included in the final model.

3.2. Functional studies

Functionality of recombinant PfTrxR was assessed by using (i) the classical DTNB assay at 20 °C, to monitor electron transfer from NADPH to the Cys88–Cys93 couple *via* the FAD, and (ii) the insulin precipitation assay, to monitor electron transfer to Trx, the macromolecular substrate.

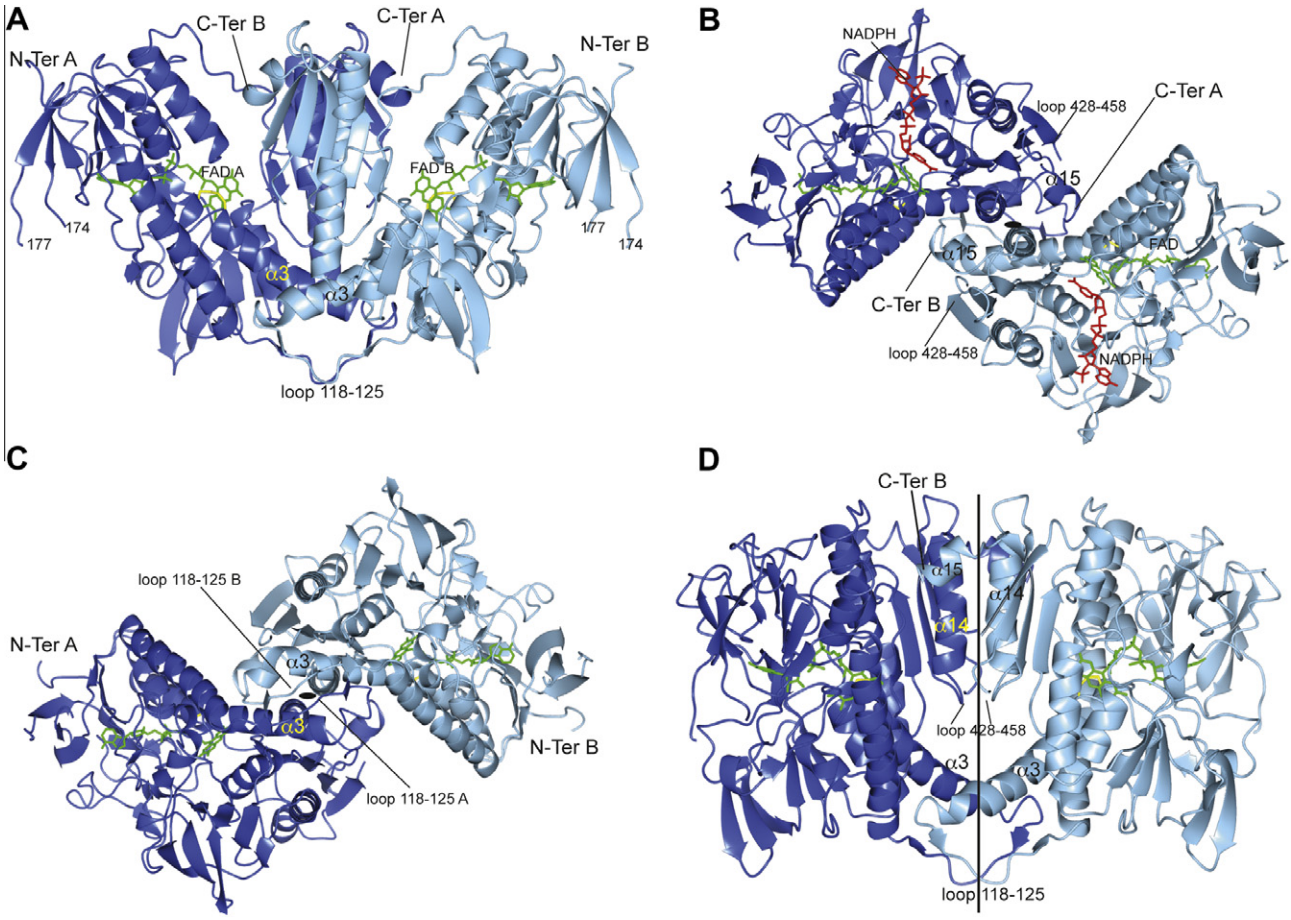

Fig. 1. Ribbon representation of the overall structure of PfTrxR. Subunit A is in blue and subunit B in light blue. In stick representation are indicated FAD (green) and Cys88–Cys93 couple of the active site (yellow). N-term and C-term of the two monomers A and B (as per crystal structure) are also labelled. The final model contains a total of 437 residues, from 38 to 174, from 177 to 427 and from 457 to 505 in each subunit. Panel A: Front view. Panel B: Top view, in which NADPH, in red, was inserted after superposition with the human enzyme (PDB ID 2ZZC [10]) and after having swung out the active site Tyr-232. Panel C: Bottom view. Panel D: Front view centered on the 2-fold axis (i.e. rotated by 30° towards the right with respect to panel A), for a better view of the central cavity. The 2-fold axis is represented either as a black stick or as an oval.

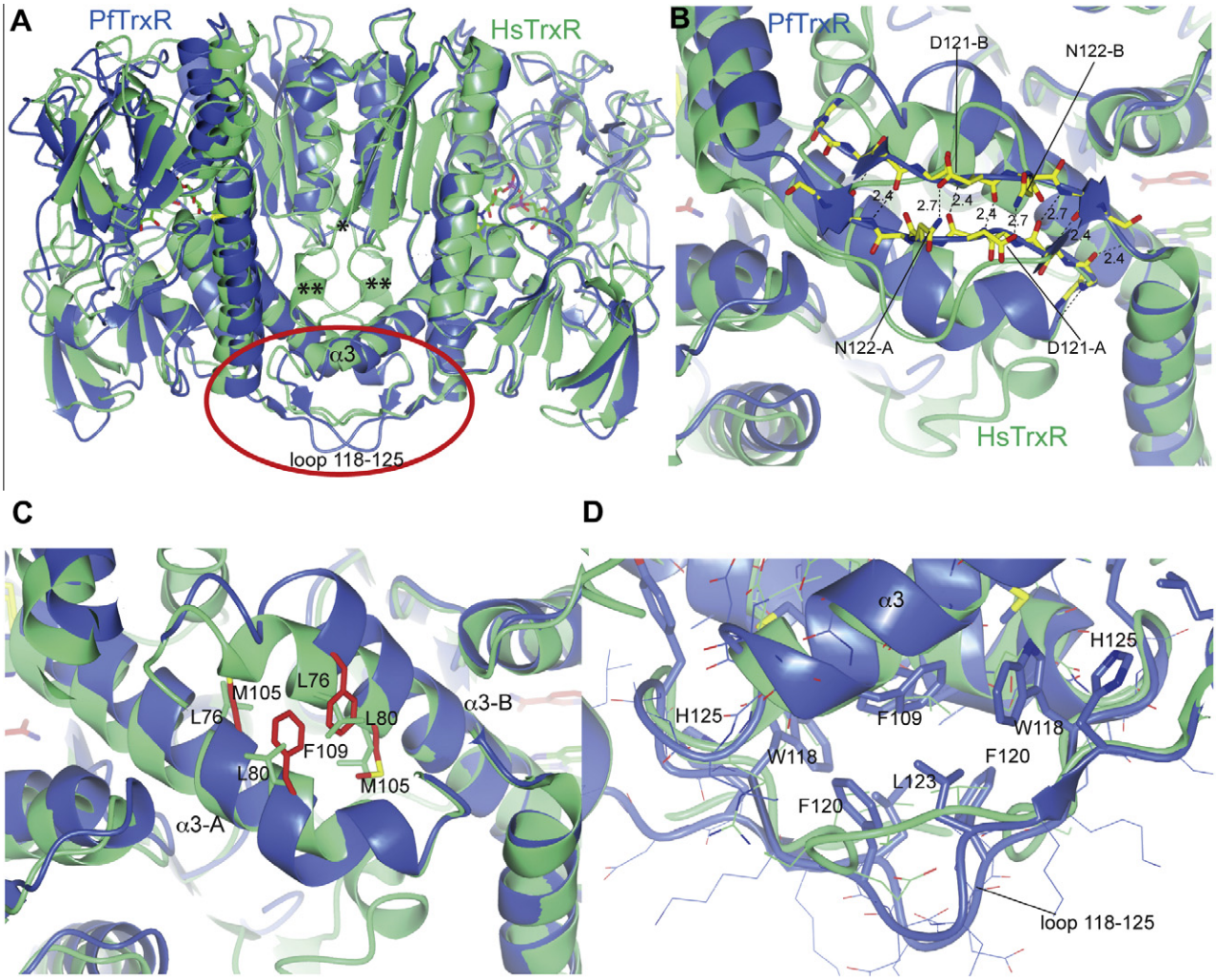

Fig. 2. Superposition of PfTrxR (blue) with HsTrxR (green). Panel A: Overall superposition in ribbon representation of the two enzymes along the dimer interface (same orientation as Fig. 1D). The red oval highlights the interface region enlarged in the next panels. *denotes the position of the C-terminal in HsTrxR; **marks the interface loop from residue 407 to 421 of HsTrxR. Panel B: Bottom view, showing the H-bond zipper stabilizing the PfTrxR antiparallel loop 118–125 from the two monomers. Main chain atoms and Asp121 and Asn122 side chains are shown in yellow stick. Distances are in Å. Panel C: Bottom view, after clipping the antiparallel loop and highlighting helices α3 belonging to the two monomers. In stick representation are shown: Met105 and Phe 109 of PfTrxR (red), Leu76 and Leu80 of HsTrxR (green). Panel D: Front view highlighting the hydrophobic cluster between helix α3 and loop 118–125 of PfTrxR.

In the first assay K_m was 240 μM and k_{cat} was 14.7 s^{-1}; in the second one the starting time was 150 s and the rate 0.68 ΔAbs min^{-1}. Both sets of data are in agreement with previously published results on the wild type enzyme [9,29].

To investigate the role of the N-terminal extension, we produced a truncated recombinant enzyme lacking the first 34 residues, in an attempt to produce crystal-prone boundaries and improve protein stability. This truncated form displayed the same enzymatic activity against DTNB and Trx as the full length enzyme (data not shown); therefore the functional role of this N-terminal domain remains unclear; unfortunately no improvement in crystal quality was observed.

4. Discussion

Thioredoxin reductase (PfTrxR) is a vital enzyme for the redox metabolism of *P. falciparum*, particularly during the erythrocytic stage of the parasite life cycle. Although the 3D structures of several mammalian proteins belonging to the same class are available, up to date Glutathione reductase is the only redox enzyme from *P. falciparum* whose structure has been solved [30]. Here we report the first crystallographic structure of PfTrxR in the oxidized form, and discuss its peculiar features by reference to human TrxR [10] and to the *in silico* models of PfTrxR recently published [11,12].

The experimental structure of PfTrxR displays several features unique to the parasite that will be useful to increase our understanding of the mechanism of binding of specific antimalarial drugs, and to unveil the dynamics of a protein belonging to Apicomplexa parasites, which spend a significant part of their lifecycle inside the red blood cell.

Despite the non-atomic resolution of the structure (2.9 Å) and the lack of electron density over three small regions of the protein (see above), we shall discuss the peculiarities of the crystallographic data since they are crucial for a rational analysis of the action of novel antimalarial drugs. This is of some immediate interest given the recent discovery of a new class of PfTrxR inhibitors [8], which are presumed to bind in the cavity next to the dimer interface. The specific features of this cavity in PfTrxR, relative to that observed in human TrxR [8,30], will be discussed in some detail.

4.1. The interface domain

As for the other TrxR enzymes, the homodimer is stabilized essentially by two interface contact regions (Figs. 1 and 2): the first comprising the last two α-helices of the C-terminal domain (the long α14 and the short α15), and the second being constituted by residues belonging to the last part of α3 and by its downstream loop (residues 118–125). It is of significance that the unstructured C-terminal arm is located in the cleft arising from these two interface regions and the FAD domain, with each C-terminal contacting the FAD domain of the partner subunit.

While the first interface region is conserved and very similar to that observed for mammalian and Apicomplexan TrxRs (Supplementary material Fig. 3), the second one is substantially different and quite peculiar. In PfTrxR helix α3 is bent due to the presence of Met105 and Phe109 (Fig. 2C), which are conserved only in the *Plasmodium* species (Supplementary material Fig. 3). These two bulky residues push the two interface helices apart, inducing a bending that triggers a conformational reorganization of the downstream loop, also part of the same interface. While in the mammalian structures these loops are open, in PfTrxR they assume an anti-parallel conformation, forming an extended and well defined H-bonding network centered on Asp121 and Asn122, which further stabilizes the interface (Fig. 2B).

In the region between α3 and the anti-parallel loops, a dense cluster of aromatic and hydrophobic residues is observed, comprising not only the above mentioned Met105 and Phe109, but also Ile108, Trp118, Phe120 and Leu123 (Fig. 2D). Overall, even though the buried surface area of the entire interface is similar to that reported for other enzymes, in PfTrxR it is stabilized by more polar contacts, yielding a dissociation energy of 31 kcal/mol *versus* 19 kcal/mol calculated for the human enzyme after removal of the C-terminal arm (residues 468–493), using PISA [31] at EBI (http://www.ebi.ac.uk/pdbe/prot_int/pistart.html). This is in agreement with the hypothesis that in PfTrxR the mobile C-terminal arm only marginally contributes to the dimer stability.

4.2. The interface cavity

The interface cavity between the two interface contact regions has often been invoked as a potential inhibitor binding site. In fact in PfTrxR it is peculiarly narrower than in HsTrxR due to the presence of Tyr101 and His104. Moreover, these residues modify the stereo-chemical properties of the interface surface, given that their counterparts in the human enzyme are, respectively, Gln and Leu (Fig. 3 and Supplementary material Fig. 3). Furthermore Tyr101 of one monomer is engaged in H-bond with Asp112 on α3 of the other monomer. Therefore both the size of this cavity and its nature are exploitable properties of the plasmodial enzymes, since they could presumably host smaller and slightly more amphipathic molecules than the human enzyme. These features might be crucial to obtain a good pharmacophoric map and achieve better selectivity.

Both published models of PfTrxR, based either on the human enzyme [11] or on the mouse enzyme [12] did not spot down these features, or they were mis-regarded by the authors. Therefore, *in silico* models based on a C-terminal arm that strengthens the interface region should be regarded as highly suspicious.

4.3. Exploitability

PfTrxR crystal structure highlighted the conservation of the binding site for Trx, which is located at the bottom of α4. Since the structure of HsTrxR in complex with HsTrx is available [32], we have superimposed this complex (PDB ID: 3QFB) to PfTrxR and indeed the contact surface area between PfTrxR and Trx is nearly identical (Figure not shown), the only substitution being Arg139, conserved in all plasmodial TrxR, that replaces Gly260 of

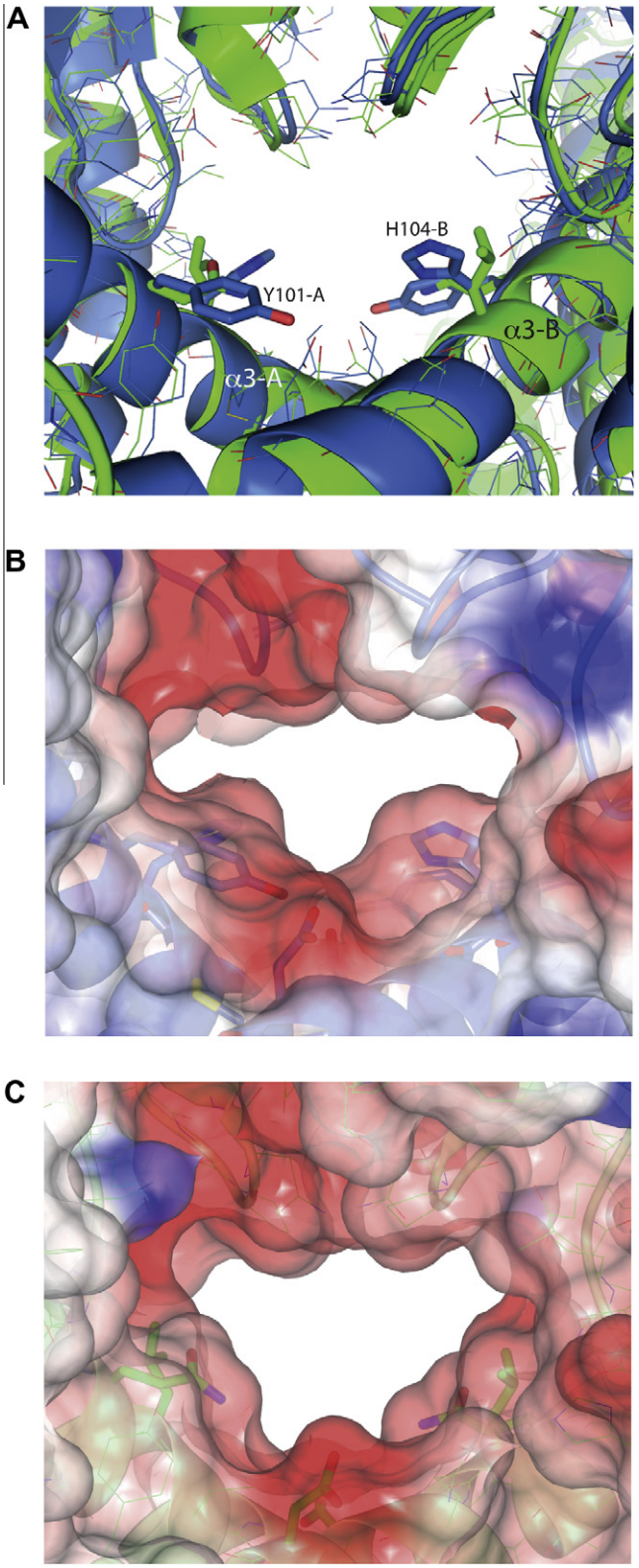

Fig. 3. The cavity of PfTrxR (blue) in comparison with HsTrxR (green). Panel A: Enlarged view of the central cavity, highlighting Tyr101 and His104 from both monomers of PfTrxR, and the corresponding Gln72 and Leu75 of HsTrxR. Panel B: Electrostatic surface of the cavity of PfTrxR. Panel C: Electrostatic surface of the cavity of HsTrxR, showed after having sliced out the loop from residue 407 to 421.

the human enzyme. This mutation is counteracted by the substitution of Thr30 of HsTrx with Glu28 of PfTrx, thus changing the interaction between the two proteins from H-bond to salt bridge. The functional conservation has been indirectly confirmed by the functional assays, where Trx from an unrelated parasite (*Schistosoma mansoni*), which has Thr as HsTrx, has been used instead of PfTrx as an electron acceptor.

Therefore we might speculate inhibitors binding in this region to be highly toxic, since they would possibly interfere with both HsTrxR and PfTrxR binding to Trx. Indeed it has been reported that an anticancer drug Terpyridine Platinum(II) inhibits the complex formation between HsTrxR and HsTrx, on top of being a topoisomerase inhibitor [10]. We can speculate that this class of compounds would not be useful as antiplasmodial agents since they would be too cytotoxic.

Very recently a paper has been published presenting two new classes of potent electrophilic non competitive inhibitors of PfTrxR [8]. The authors hypothesize that these compounds might bind in the interface domain. In light of our results, indeed the differences in the interface cavity between the parasite and human enzyme could be exploited for selecting specific drug compounds.

In conclusion, PfTrxR structure has revealed unique unexpected features on top of a conserved 3D-fold. This enzyme displays a more stable monomer–monomer interface and an extended and well defined H-bonding network along the loop 118–125 of both subunits, both features being absent in the human enzyme. The greater stability of the dimer in the parasite could partially compensate for the more extended structural flexibility, largely due to the loop 429–458 and the C-terminal arm. Relevant questions remain presently unanswered such as: why the *Plasmodium* species evolved such a diverse interface and what the evolutionary advantage of these flexible insertions might be.

5. Accession numbers

Coordinates and structure factors have been deposited in the Protein Data Bank with accession number 4B1B.

Acknowledgments

We would like to thank Prof. Robert Hondal and Dr. Gregg Snider (University of Vermont, USA) for helpful discussion. The research leading to these results has received funding from: Fondazione Roma under Grant "Rational approach to the specific inhibition of *Plasmodium falciparum* and *Schistosoma mansoni*" to MB; MIUR of Italy under Grant FIRB RBRN07BMCT_007 to MB and International FIRB RBIN06E9Z8 to AB; "Sapienza" University of Rome under Grants "Progetti di Università" 2010 and 2011 to AB; the European Community's Seventh Framework Programme (FP7/2007-2013) under Grant agreement no.226716 to AEM. GG is a supported fellow of Fondazione Roma.

Appendix A. Supplementary data

Supplementary data associated with this article can be found, in the online version, at http://dx.doi.org/10.1016/j.bbrc.2012.07.156.

References

[1] World Health Organization. World Malaria Report 2011. (2011). Available online at http://www.who.int/malaria/world_malaria_report_2011/en.

[2] S.M. Kanzok, R.H. Schirmer, I. Turbachova, R. Iozef, K. Becker, The thioredoxin system of the malaria parasite *Plasmodium falciparum*. Glutathione reduction revisited, J. Biol. Chem. 275 (2000) 40180–40186.

[3] S. Müller, Thioredoxin reductase and glutathione synthesis in *Plasmodium falciparum*, Redox Rep. 8 (2003) 251–255.

[4] C. Nickel, S. Rahlfs, M. Deponte, S. Koncarevic, K. Becker, Thioredoxin networks in the malarial parasite *Plasmodium falciparum*, Antioxid. Redox Signal. 8 (2006) 1227–1239.

[5] S. Müller, Redox and antioxidant systems of the malaria parasite *Plasmodium falciparum*, Mol. Microbiol. 53 (2004) 1291–1305.

[6] N.H. Hunt, R. Stocker, Oxidative stress and the redox status of malaria-infected erythrocytes, Blood Cells 16 (1990) 499–526.

[7] J.F. Turrens, Oxidative stress and antioxidant defenses: a target for the treatment of diseases caused by parasitic protozoa, Mol. Aspects Med. 25 (2004) 211–220.

[8] A.J. Theobald, I. Caballero, I. Coma, G. Colmenarejo, C. Cid, F.J. Gamo, M.J. Hibbs, A.L. Bass, D.A. Thomas, Discovery and biochemical characterization of *Plasmodium* thioredoxin reductase inhibitors from an antimalarial set, Biochemistry 51 (2012) 4764–4771.

[9] P.J. McMillan, L.D. Arscott, D.P. Ballou, K. Becker, C.H. Williams Jr., S. Müller, Identification of acid-base catalytic residues of high-Mr. Thioredoxin reductase from *Plasmodium falciparum*, J. Biol. Chem. 281 (2006) 32967–32977.

[10] Y.C. Lo, T.P. Ko, W.C. Su, T.L. Su, A.H. Wang, Terpyridine-platinum(II) complexes are effective inhibitors of mammalian topoisomerases and human thioredoxin reductase 1, J. Inorg. Biochem. 103 (2009) 1082–1092.

[11] A.K. Banerjee, N. Arora, U.S. Murty, Structural model of the *Plasmodium falciparum* thioredoxin reductase: a novel target for antimalarial drugs, J. Vector Borne Dis. 46 (2009) 171–183.

[12] A. Caroli, S. Simeoni, R. Lepore, A. Tramontano, A. Via, Investigation of a potential mechanism for the inhibition of SmTGR by auranofin and its implications for *Plasmodium falciparum* inhibition, Biochem. Biophys. Res. Commun. 417 (2012) 576–581.

[13] U. Mueller, N. Darowski, M.R. Fuchs, R. Förster, M. Hellmig, K.S. Paithankar, S. Pühringer, M. Steffien, G. Zocher, M.S. Weiss, Facilities for macromolecular crystallography at the Helmholtz-Zentrum Berlin, J. Synch. Rad. 19 (2012) 442–449.

[14] W. Kabsch, XDS, Acta Crystallogr. D: Biol. Crystallogr. 66 (2010) 125–132.

[15] A.J. McCoy, R.W. Grosse-Kunstleve, P.D. Adams, M.D. Winn, L.C. Storoni, R.J. Read, Phaser crystallographic software, J. Appl. Cryst. 40 (2007) 658–674.

[16] Collaborative Computer Project number 4, The CCP4 Suite: Programs for Protein Crystallography, Acta Crystallogr. D: Biol. Crystallogr. 50 (1994). 760–763.

[17] M.D. Winn, C.C. Ballard, K.D. Cowtan, E.J. Dodson, P. Emsley, P.R. Evans, R.M. Keegan, E.B. Krissinel, A.G. Leslie, A. McCoy, S.J. McNicholas, G.N. Murshudov, N.S. Pannu, E.A. Potterton, H.R. Powell, R.J. Read, A. Vagin, K.S. Wilson, Overview of the CCP4 suite and current developments, Acta Crystallogr. D: Biol. Crystallogr. 67 (2011) 235–242.

[18] E.I. Biterova, A.A. Turanov, V.N. Gladyshev, J.J. Barycki, Crystal structures of oxidized and reduced mitochondrial thioredoxin reductase provide molecular details of the reaction mechanism, Proc. Natl. Acad. Sci. USA 102 (2005) 15018–15023.

[19] R.A. Nicholls, F. Long, G.N. Murshudov, Low-resolution refinement tools in REFMAC5, Acta Crystallogr. D: Biol. Crystallogr. 68 (2012) 404–417.

[20] P. Emsley, B. Lohkamp, W. Scott, K. Cowtan, Features and development of coot, Acta Crystallogr. D: Biol. Crystallogr. 66 (2010) 486–501.

[21] V.B. Chen, W.B. Arendall 3rd, J.J. Headd, D.A. Keedy, R.M. Immormino, G.J. Kapral, L.W. Murray, J.S. Richardson, D.C. Richardson, MolProbity: all-atom structure validation for macromolecular crystallography, Acta Crystallogr. D: Biol. Crystallogr. 66 (2010) 12–21.

[22] R.A. Laskowski, M.W. MacArthur, D.S. Moss, J.M. Thornton, PROCHECK: a program to check the stereochemical quality of protein structures, J. Appl. Cryst. 26 (1993) 283–291.

[23] S. McNicholas, E. Potterton, K.S. Wilson, M.E. Noble, Presenting your structures: the CCP4mg molecular-graphics software, Acta Crystallogr. D: Biol. Crystallogr. 67 (2011) 386–394.

[24] M.A. Larkin, G. Blackshields, N.P. Brown, R. Chenna, P.A. McGettigan, H. McWilliam, F. Valentin, I.M. Wallace, A. Wilm, R. Lopez, J.D. Thompson, T.J. Gibson, D.G. Higgins, Clustal W and Clustal X version 2.0, Bioinformatics 23 (2007) 2947–2948.

[25] E.S. Arnér, L. Zhong, A. Holmgren, Preparation and assay of mammalian thioredoxin and thioredoxin reductase, Methods Enzymol. 300 (1999) 226–239.

[26] A. Holmgren, Thioredoxin catalyzes the reduction of insulin disulfides by dithiothreitol and dihydrolipoamide, J. Biol. Chem. 254 (1979) 9627–9632.

[27] L. Slabinski, L. Jaroszewski, L. Rychlewski, I.A. Wilson, S.A. Lesley, A. Godzik, XtalPred: a web server for prediction of protein crystallizability, Bioinformatics 23 (2007) 3403–3405.

[28] D.W. Buchan, S.M. Ward, A.E. Lobley, T.C. Nugent, K. Bryson, D.T. Jones, Protein annotation and modelling servers at University College London, Nucl. Acids Res. 38 (Suppl) (2010) W563–W568.

[29] T.W. Gilberger, R.D. Walter, S. Müller, Identification and characterization of the functional amino acids at the active site of the large thioredoxin reductase from *Plasmodium falciparum*, J. Biol. Chem. 272 (1997) 29584–29589.

[30] G.N. Sarma, S.N. Savvides, K. Becker, M. Schirmer, R.H. Schirmer, P.A. Karplus, Glutathione reductase of the malarial parasite *Plasmodium falciparum*: crystal structure and inhibitor development, J. Mol. Biol. 328 (2003) 893–907.

[31] E. Krissinel, K. Henrick, Inference of macromolecular assemblies from crystalline state, J. Mol. Biol. 372 (2007) 774–797.

[32] K. Fritz-Wolf, S. Kehr, M. Stumpf, S. Rahlfs, K. Becker, Crystal structure of the human thioredoxin reductase-thioredoxin complex, Nat. Commun. 2 (2011) 383.